Carbohydrate Polymers **22** (1993) 153–160

Hydration characteristics of the cross-linked hyaluronan derivative hylan

Shoji Takigami, Machiko Takigami

Department of Chemistry, Gunma University, Japan

&

Glyn O.Phillips*

Newtech Innovation Centre, The North East Wales Institute, Clwyd, Wales, UK

(Received 6 May 1993; revised version received 16 June 1993; accepted 17 June 1993)

The ability of hylan, the formaldehyde cross-linked derivative of hyaluronan, to interact with water has been studied using differential scanning calorimetry (DSC). Three types of water can be distinguished: *non-freezing*, *freezing-bound* and *free*. When the water content of the system is increased, even by up to 10%, almost all the water remains in the freezing-bound state, with a ΔH value less than free water. Several metastable states of water can be detected within the structured hylan–water matrix, indicative of defects in the frozen-bound ice structure. The maximum amount of non-freezing water, intimately associated with the hydrophilic groups of hylan, corresponds to 13 mol water per disaccharide unit of the hyaluronan chain. The large capacity shown by hyaluronan entangled networks to build water into their structure could also be responsible for their unusually high viscosity and elasticity after the onset of entanglement. Such viscoelastic properties are the basis for their use in viscosupplementation of arthritic diseased joints.

INTRODUCTION

Hyaluronan (Hyaluronic acid) is a glycosaminoglycan found extensively in connective tissue. It is a straight-chain polymer consisting of alternating $\beta(1\rightarrow4)$ linked 2-acetamide-2-deoxy-D-glucose and $\beta(1\rightarrow3)$ linked D-glucuronic acid. In its purest, non-inflammatory form, it is extensively used as a viscosurgical tool in ophthalmology, and is now being introduced for the treatment of traumatic arthritis in horses and humans (Balazs, 1968; Laurent, 1987; Balazs & Denlinger, 1989). The major property of hyaluronan, which underpins its therapeutic usefulness, is its ability to interact with water to form viscoelastic matrices (Balazs & Leshchiner, 1989). Recently, cross-linked derivatives of hyaluronan have been prepared, with molecular weights up to 23×10^6 Da, which are soluble in water to give extremely viscoelastic solutions (Balazs & Leshchiner, 1989). Such hylan hydrogels have been shown to be highly biocompatible, non-antigenic, non-inflammatory, and non-tissue reactive (Balazs & Leshchiner, 1986). The rheological properties of hylan in water are quite different from those of hyaluronan at the same concentration. At the lowest frequencies and shear rates, the elasticity and the shear and dynamic viscosities are significantly higher for hylan than the corresponding hyaluronan solutions. It has been stated that the reason for this difference is that the interactions with the solvent water are different for the two polysaccharides (Balazs & Leshchiner, 1989).

The state of water in various water–polyelectrolyte systems has been extensively studied using differential scanning calorimetry DSC) (Hatakeyama *et al.*, 1985*a, b, c*; Hatakeyama, *et al.*, 1987*a, b, c, d, e*; Nakamura *et al.*, 1987; Yoshida *et al.*, 1989). We have, therefore, applied their method to hylan in order to establish whether the unusual rheology can be related to the ability of hylan to interact with water. Moreover, we seek to assess whether the hyaluronan framework structure confers upon its derivative, hylan, the ability to 'bind' water more than other polysaccharides and related polyelectrolytes.

*To whom correspondence should be addressed.

Carbohydrate Polymers 0144-8617/93/$06.00

Thermal, dielectrical and spectroscopic methods have been used to study the state of water in aqueous polymer systems (Uedaira, 1975; Wise & Pfeffer, 1987; Mauritz & Fu, 1988). In polysaccharide hydrogels, three types of water have been distinguished: non-freezing water; freezing-bound water and free water. When examined by DSC, the free water shows a sharp endothermic peak on melting at a temperature (T_m) identical with pure water. Freezing-bound water, on the other hand, melts at lower temperatures, showing a broad endothermic transition. When W_c is defined as the amount of water (in g) compared with the dry weight of the sample (in g), then T_m for the freezing-bound water increases with increasing W_c. For the free water, T_m is independent of W_c and the thermal history of the system. The distinctiveness of freezing-bound water is further illustrated by its 10-times slower cystallisation rate, compared with free water (Yoshida *et al.*, 1989). The non-freezing water shows no first-order transition either on heating or cooling, but shows a glass transition, particularly when associated with linear polymers.

Here we apply the DSC method to hylan hydrogels, which allows us to classify the types of water present and demonstrates their extraordinary capacity to 'bind' water in the freezing-bound form.

EXPERIMENTAL

The formaldehyde cross-linked hylan derivative (Balazs & Leshchiner, 1986) was supplied by Dr Endre A. Balazs (Biomatrix Inc. USA) in solid form. One sample had been freeze dried from the fluid, and the other precipitated with isopropanol and dried in a vacuum oven at 55°C. We observed no difference in the behaviour of the two samples. In an independent investigation, we used a variety of methods, including gel permeation chromatography, low-angle and multi-angle laser light scattering to characterise the samples. The molecular weight was 6×10^6 Da with a polydispersity of ~4. For reference also, we retained a sample of sodium hyaluronan, provided by Denki Kagaku Kogyo Kabushiki Kaisha produced by *Streptococcus equi.* (M_w $1{\cdot}55 \times 10^6$ Da).

The high performance gel permeation chromatograms were determined using a Beckman Instruments System Gold 126 Programmable Solvent Module/166 Programmable Detector Module HPGPC apparatus fitted with a 'ready-to-use' stainless steel column SG-10-6000 NH_2 (8 × 250 ID) filled with amino-propyl modified highly porous silica gel derivative. A 20 μl manual sample loop was used for introducing the samples to the column and the elution buffer flow rate was maintained at 0·5 cm^{-3} min^{-1}. The eluent stream was analysed by UV absorption at 206 nm and the chromatograms recorded using a CR6A chromatograph Integrator Chromatopac (Shimadzu, Japan). All measurements were performed at room temperature.

Additionally, the weight average molecular weight was determined by low-angle (5–7°) laser light-scattering using a Chromatix KMX6 instrument. Samples were filtered through an on-line 0·4 micro Millipore Filter immediately prior to being introduced into the measuring cell. A test run with a 0·8 micro Filter gave the same result. Samples were made 0·05 M in $NaClO_4$, before measuring. Values of 1·34 and 0·16 were taken for the refractive index (n) and dn/dc respectively, where c is the hylan concentration in g cm^{-3}.

Finally, the weight average molecular mass, radius of gyration, and second virial coefficients of the various samples were determined by MALLS using the Malvern dual function 7027 digital correlator equipped with a helium–neon laser light source (λ = 632·8 nm) with a maximum power output of 15 mW.

Differential Scanning Calorimetry (DSC)

Samples weighing 0·1–3 mg were mixed with distilled water in aluminium pans, which had been previously treated with water in an autoclave at 110°C for 3 h in order to eliminate any reaction between the aluminium surface and water. In order to adjust the water content of the samples, excess water was removed slowly in a dessicator containing 50% aqueous H_2SO_4 at room temperature (relative humidity *c.* 35%). The pans were subsequently sealed hermetically.

A Perkin Elmer DSC II, equipped with cooling apparatus was used to measure the phase transition of sorbed water in the samples, which were cooled from 303K to 150K at 10K/min and subsequently heated to 303K at 10K/min. The transition temperatures are defined as the peak-top temperatures as given by the DSC heating curves. The temperature scale and heat of fusion were calibrated using distilled water as the standard material (Yoshida *et al.*, 1989).

Water Content

After DSC measurements, the sample pans were pricked with a pin to remove water from the samples, which were thereafter dried *in vacuo* for 30 min at 100°C, then left overnight at 50°C. After weighing the water content was determined:

$$W_c\ (g/g) = \frac{\text{Weight of water (in g) in hylan}}{\text{Weight of dry hylan (in g)}}$$

The following designations are used for the weights of the various types of water: W_{nf}, non-freezing, W_{fb}, freezing-bound and W_w free water. The DSC heating curves show distinct and separate transitions for two types of freezing-bound water (W_{fb1} and W_{fb2}) and free water (W_w), which enabled these quantities to be calcu-

lated from the areas represented by the endothermic transitions. The weight of non-freezing was then obtained from the expression:

$$W_c = W_{nf} + W_{fb} + W_w$$

RESULTS AND DISCUSSION

DSC heating curves are shown in Fig. 1. The W_c values are listed, and it is immediately evident that the melting behaviour of the water is related to the water content of the samples. The dry polysaccharide showed no transition over the temperature range of the experiments. Below a W_c value of 0·5 there is no observable transition. However, as W_c is increased, three endothermic peaks can be observed. One relates to freezing-bound water near 250K (T_{fb2}), a broad transition due to the major portion of the freezing-bound water (T_{fb1}), and the third due to the melting of free water (T_w). Figure 1 shows that the peak at T_{fb1} moves to higher temperatures and broadens with increasing W_c. Individual transitions can also be discerned within the broadening peak (see, for example, W_c 1·66 in Fig. 1), which points to various thermodynamic states of the freezing-bound water within the hylan hydrogel system. Such multi-peak behaviour is indicative of various frozen states of water, but which are different from normal ice with ice I structure (Franks, 1972; Hatakeyama & Nakamura, 1988). The effects of varying W_c on the T_w, T_{fb1} and T_{fb2} are shown in Fig. 2. When W_c approaches 10, T_{fb1} has moved almost completely to 273K, the melting peak temperature of free water (T_w). However, even in this high water content, effectively a 10% aqueous solution, the large majority of the water molecules remain in the frozen-bound state. The shoulder directly corresponding to T_w is still distinct (see $W_c \sim 9$, Fig. 1), although there is overlap between the two transitions. Here, the water in its behaviour is approaching that of free water.

The endothermic transition at T_{fb2} does not change its position significantly with increasing W_c (Fig. 2). Although freezing, this water is held within the matrix, and is largely immobile. Whereas the bound water molecules first act to disrupt hydrogen bonds in the solid, in the first instance bridges with OH-bonded water molecules can provide some stability for the next layer of water molecules. This water appears to have a structure intermediate between non-freezing water and the bulk of freezing-bound water, thus reducing its mobility (Nakamura *et al.*, 1983). As W_c increases, sorption of the water continues readily. The three-dimensional network of polysaccharide and water continues to build up as a structured entity, and retains its distinctive character different from free water until $W_c > 10$. At $W_c \sim 13$, only the free water transition is observable (Fig. 1).

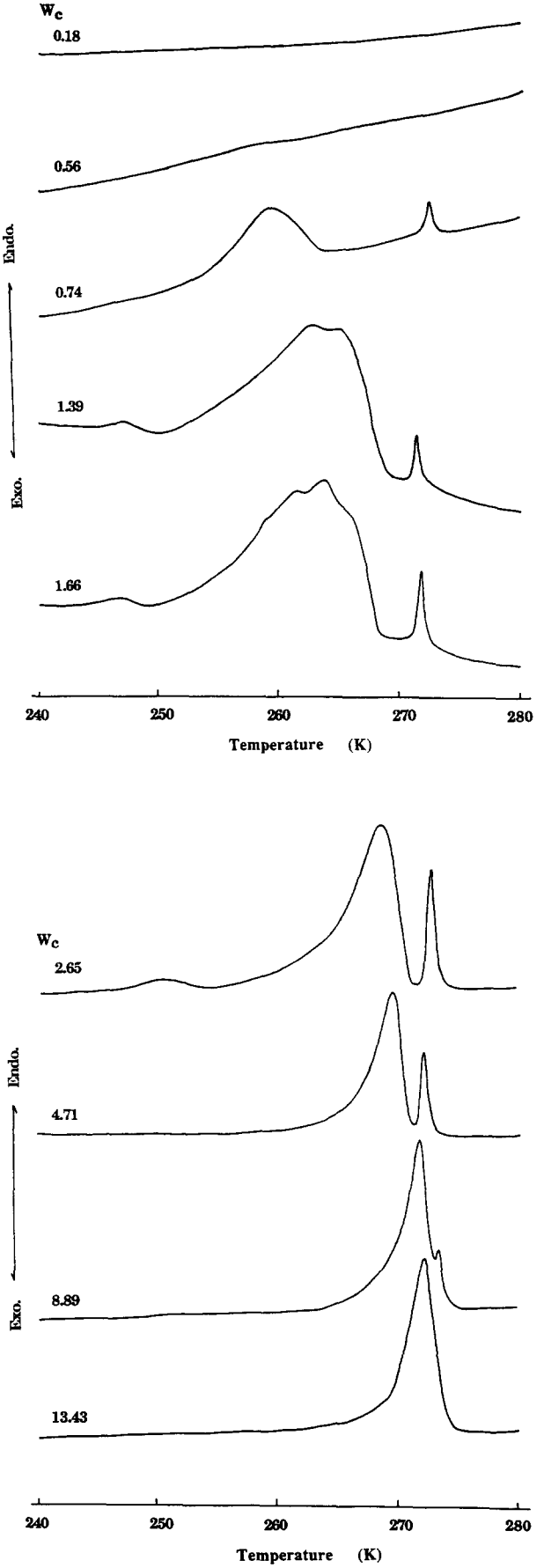

Fig. 1. DSC heating curves for water–hylan systems.

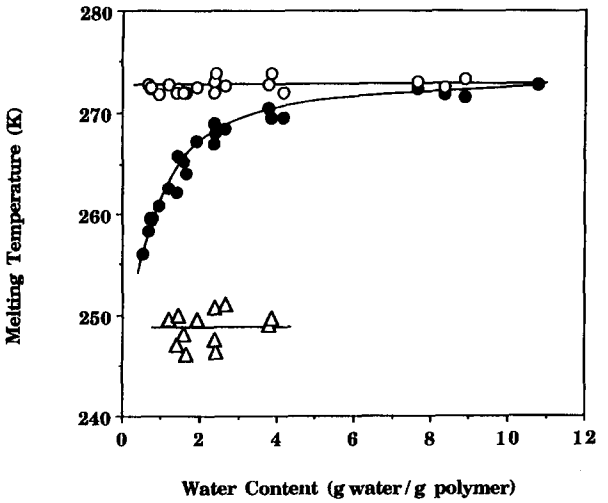

Fig. 2. Variation of melting temperature with water content. (○) free water (T_w); (●) bound water (T_{fb1}); (△) bound water (T_{fb2}).

We have also compared the behaviour on cooling with the heating cycle. Figure 3 illustrates the difference between the two cycles. Two situations can be distinguished. At a W_c value below 0·8, when the system is cooled, no exothermic transition due to the crystallisation of the ice is evident. However, when this system is subsequently heated, there is first a small exothermic transition followed by a larger endothermic change. This behaviour has previously been encountered (Hatakeyama *et al.*, 1987*c*; Nakamura *et al.*, 1987; Yoshida *et al.*, 1989), and can be explained by initial formation of amorphous ice on cooling, which on heating first crystallises exothermically from the glassy state, and subsequently melts endothermically. Such cold crystallisation results in a more organised bound state which then melts as frozen-bound water. At W_c values above 0·8, there is sufficient ice produced on cooling to enable us to observe both exothermic crystallisation and endothermic melting as the cooling and heating cycles progress. In each instance, ΔH (melting) is greater than ΔH (crystallisation), as shown in Fig. 4, an increment which decreases with W_c. The freezing-bound water is distinguishable thermodynamically from free water, and even at the highest values of W_c, where a distinctive freezing-bound transition is discernable from free water ($W_c \sim 10$), the bound state continues to exert a dominant influence on the melting process, with the enthalpy remaining less than the value of 79·8 cal/g of free water. Figure 5 shows the variation in bound water ($W_{fb1} + W_{fb2}$), total freezing water ($W_{fb1} + W_{fb2} + W_w$), non-freezing water (W_{nf}) and free water (W_w) with W_c. Since the weight of the various types of water is calculated from the heat of fusion of water, a slope of one in Fig. 5 for total water would indicate the enthalpy of melting of the water to be 79·8 cal/g, as for free water. The slope, however, is less than one, indicating that the enthalpy of melting for the water remains less than free water, due to defects in the freezing-bound ice, up to the W_c value of ~10. The structure of freezing-bound water remains distinct from the conventional structure of hexagonal ice (Nakamura *et al.*, 1983).

However, the most distinctive feature of Fig. 5 and of this study is the enormous capacity of hylan to bind water, and modify its freezing behaviour. In Table 1, we compare the relative ability of various polymer systems

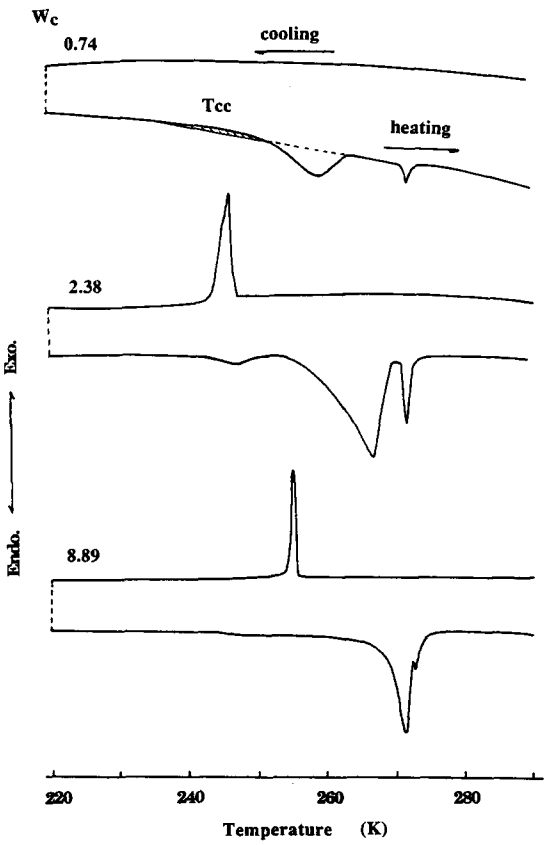

Fig. 3. DSC heating and cooling cycles for hylan–water systems at different W_c values.

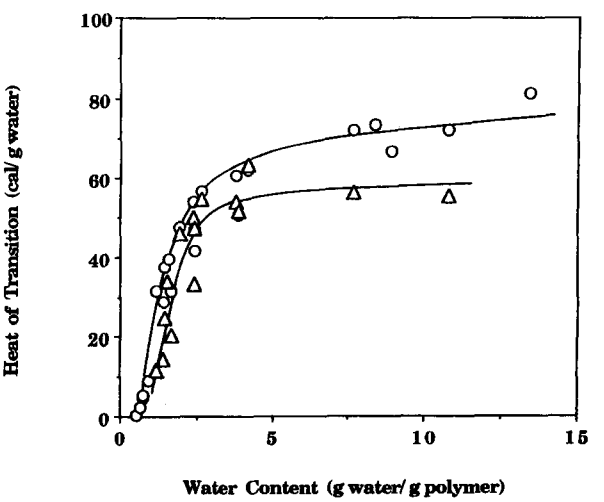

Fig. 4. Variations in heat of transition with water content. (○) heat of fusion; (△) heat of crystallisation.

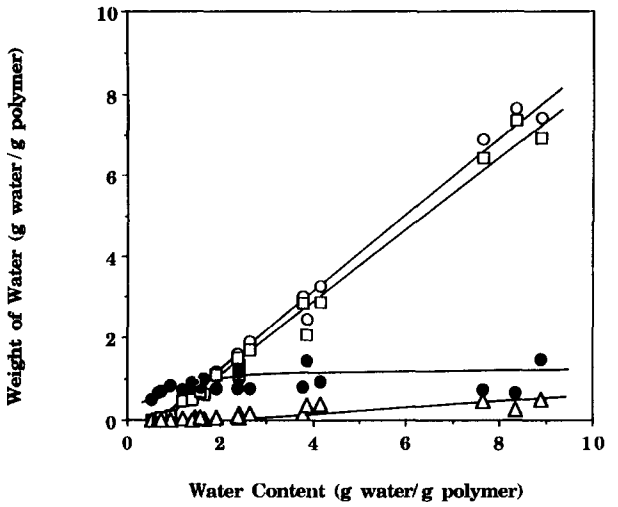

Fig. 5. Variation in content of the various types of sorbed water with water content. (○) total freezing water (bound and free) ($W_w + W_{fb1} + W_{fb2}$); (□) bound water ($W_{fb1} + W_{fb2}$); (△) free water (W_w); (●) non-freezing water (W_{nf}).

to bind water by quoting the values of W_c where saturation occurs, and no further bound water is distinguishable. Hylan is in a different category to all others studied, and more than three times more effective than the previously quoted value for hyaluronic acid. It is five times more effective than xanthan, used extensively as a water binder in food stabilisation systems. In our preliminary studies on hyaluronic acid itself to W_c values up to ~1·7, there are indications of a comparable ability to bind water. We are unable to determine at this time that this ability extends to W_c values as high as ~10 for hylan.

Further observations point to metastable states of water existing as the structured hylan–water builds up with increasing amounts of water. If the cooling and heating cycles illustrated in Fig. 3 are repeated immediately after one another, then the amount of free water increases and the amount of bound water decreases. This behaviour is shown in Fig. 6(A), together with the curves obtained after annealing for 4–5 h by standing at room temperature. As the heating and cooling cycles are repeated (a to b), it is evident from the curves that the proportion of freezing-bound water decreases. On the other hand, there is no change in the proportions of free and bound water for the later instance (c to d). We have quantified this graphically in Fig. 6(B), and the computed values for free and bound water are shown.

Previously, we drew attention to the presence of a number of such states of water resulting in a number of peaks in the endothermic transition during the melting of the frozen-bound water (Fig. 1). Defects present in the frozen-bound ice structure can lead to easier melting, but the network appears to stabilise on annealing, leading to the absence of such metastable states on further cooling and heating cycles.

For certain polysaccharides, including hyaluronic acid, below W_c (as defined in Table 1) a glass transition has been reported (Yoshida *et al.*, 1989). This does not show as a discrete transition, but rather can be detected by a shift in the base line. This transition has been attributed to non-freezing water held tightly by the hydrophilic groups (OH particularly and hydrated counterions for polyelectrolytes). The temperature at which this transition occurs changes with increasing water content, and this behaviour has been attributed to a plasticizing effect of the non-freezing water in association with the increased mobility of the polymer chains. We have not found this base line deviation at *c.* 200K, which might be due to the cross-linked nature of the hylan–water system. Other cross-linked polymers, for example rubber and cross-linked resins, also do not show this transition, since the mobility of the individual chain segments is restricted. A tightly bound H-bonded matrix would also be analogous to cross-linking in its restriction of the mobility of bound water molecules. The amount of non-freezing water does not increase with water content after complete hydration of the sugar skeleton (Fig. 5(A)). From the constant value of W_{nf} and the intercept of the heat of fusion to the water content axis (W_{nf} = 0·62/g of polymer), it can be calculated that 13 mol water are bound in the non-frozen state to each disaccharide unit of hylan. This value is in

Table 1. Weight content (W_c in g/g) of water in various polymers necessary to achieve saturation

Sample	W_c	Ref.
Poly (2-hydroxystyrene)	0·080	Hatakeyama *et al.*, 1988
Poly (2-acetoxystyrene)	0·026	Hatakeyama *et al.*, 1988
Cellulose I	0·05	Hatakeyama *et al.*, 1987*a–e*
Cellulose II	0·06	Hatakeyama *et al.*, 1987*a–e*
Sodium carboxymethyl cellulose	0·08	Nakamura *et al.*, 1982
Sodium polystyrene sulphonate	1·3	Hatakeyama *et al.*, 1985*a–c*
Sodium cellulose sulphate	1·4	Hatakeyama *et al.*, 1987*a–e*
Sodium xanthan	2·0	Yoshida *et al.*, 1989; Yoshida *et al.*, 1990
Hyaluronan	3·0	Yoshida *et al.*, 1989
Hylan	10·0	This study

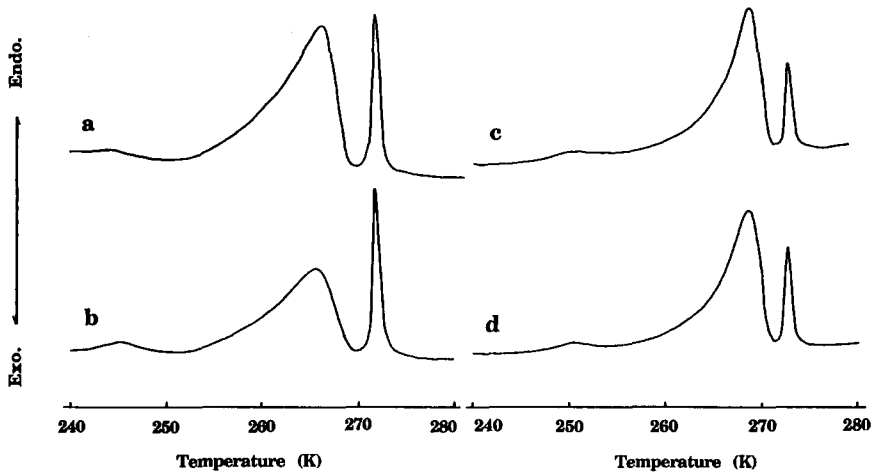

(A)

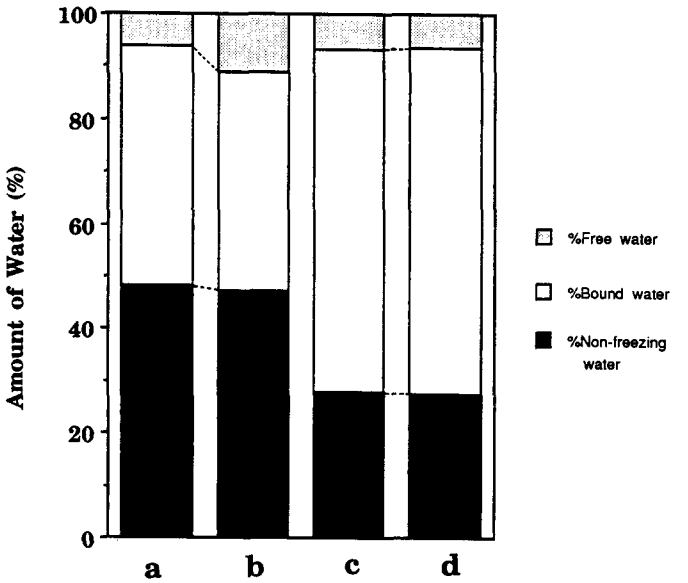

(B)

Fig. 6 (A) DSC heating and cooling cycles for hylan–water systems: a and b, repeated immediately, $W_c = 2{\cdot}4$; c and d, repeated after 4–5 h, $W_c = 2{\cdot}65$. (B) Effect of repeated heating and cooling cycles on sorbed water: a and b, repeated immediately, $W_c = 2{\cdot}4$: c and d, repeated after 4–5 h, $W_c = 2{\cdot}65$.

good agreement with the 30 mol per tetrasaccharide unit quoted previously for hyaluronic acid (Yoshida *et al.*, 1989), which, of course, contains the same basic structure as hylan.

Previously, we utilised compressibility and high-precision densimetric measurements to study the hydration of sodium hyaluronate (Davies *et al.*, 1982; 1983). It was found that the hydration of the glucuronate residue is significantly more than that of the *N*-acetyl glucosamine residue, with an average value of one molecule of water of hydration per *N*-acetylglucosamine residue and 11·3 molecules of water of hydration per sodium glucuronate residue. This gives an average value of 12·3 molecules of water of hydration per saccharide pair. If the hydration parameters of reasonably high molecular weight HA ($M_w > 5 \times 10^4$ to $3{\cdot}22 \times 10^6$) are compared with those of *N*-acetylglucosamine and sodium glucuronate and comparable concentrations (approx. 10 mM in each saccharide residue), a value of nine molecules per disaccharide unit is obtained for HA and 14·1 molecules of water of hydration per saccharide pair. This would suggest that some five molecules of water of hydration are lost on forming the two glycosidic links associated with polymer formation, from which it can be inferred that on average, approximately one molecule of water of hydration is associated with each of two anomeric hydroxy groups and one each with the C-3 in *N*-acetylglucosamine and C-4 in glucuronic acid. For a sodium hyaluronate disaccharide, the average hydration value is 11·5 water molecules

per disaccharide residue. Thus the value we have measured of 13 water molecules per disaccharide unit would indicate saturation capacity of the individual monomers to bind water. This capacity can only be achieved in the almost solid-state systems we have studied, where conditions for hydrogen bonding would be more favourable than for the dilute solutions where the compressibility measurements were undertaken. However, the agreement with the compressability values, considering the diversity of the techniques, is encouraging.

Our results, therefore, support the view that the hylan derivative we have studied readily forms structured networks with water. There is no precise information about the detailed structure of this hylan. Formaldehyde was used at neutral pH to produce a permanent bond between C-OH groups of hyaluronan chains and the amino or imino groups of a protein, which is associated with the native hyaluronan (Balazs *et al.*, 1987). This protein forms a bridge between two hyaluronan chains. Under the most appropriate conditions 2–8 hyaluronan chains can be cross-linked, giving a weight average molecular weight of between 0·8 and $2{\cdot}4 \times 10^7$ Da. Our measurements point to a somewhat lower M_w of some 6×10^6 Da, although higher molecular aggregates are also present. The cross-linking process produces a microgel which is extremely viscoelastic in water, with a viscosity at low shear rates some 10 times greater than hyaluronan of 4×10^6 Da (Balazs *et al.*, 1989). It is this high viscosity which is responsible for its long residence time in connective tissue compartments when used for viscosupplementation therapy (Balazs *et al.*, 1988).

From a physical standpoint, therefore, hylan can be regarded as two or more hyaluronan (HA) chains drawn into closer physical contact than they would be in HA itself. In aqueous solution terms, our studies have been conducted at extremely high solute concentrations (ranging from 0·5 g H_2O/g hylan to 10 g H_2O/g hylan). Even in dilute (1%) solutions, HA is believed to form a highly entangled network if the molecular weight is more than $1{\cdot}6 \times 10^6$ Da (Morris *et al.*, 1980; Arnott *et al.*, 1983; Bolliner & Wik, 1987; Yanaki & Yamaguchi, 1990). Using rubber elasticity theory to interpret the rheological of 1% HA aqueous solutions, the molecular length between entangled chains was calculated to be 0·4 μm. Since this value is considerably smaller than for synthetic polymers, it was inferred that the network in HA is formed by intermolecular hydrogen bonds. Such interactions were also considered to be responsible for the viscoelastic properties of HA solutions. From their results Yanaki and Yamaguchi (1990) related η_0, the zero shear viscosity, to M_v, the viscosity average molecular weight. Entanglement initially occurs at $M_v \sim 3{\cdot}5 \times 10^5$. Below this critical molecular weight, η_0 is proportional to $M_v^{1{\cdot}0}$, and above to $M_v^{3{\cdot}4}$. Thus from the point of view of η_0, entanglement can be detected. On the basis of the steady state shear compliance J_e°, the formation of the network of HA chains, that is elastic, starts only for molecular weights above 1×10^6 Da at 1%. Such network formation is completed at $M_v \sim 1{\cdot}60 \times 10^6$ with $\eta_0 \propto M_v^{3{\cdot}4}$ and $J_e^\circ \sim$ constant. From this point onwards, the destruction of the original intermolecular structure, and orientation of the individual chains are at the steady state and in dynamic equilibrium. The HA concentration would also exert a profound influence on the onset and maintenance of the hydrogen-bonded network. Rinaudo (Fouissac *et al.*, 1992) has similarly studied the rheological behaviour of HA over various molecular weights and concentration ranges and established a model for HA. These workers found the relationships:
In the dilute regime

$$\eta_{sp} \propto C^{1{\cdot}2} M^{1{\cdot}0} \propto (C[\eta])^{1{\cdot}2}$$

and after entanglement in the concentrated regime

$$\eta_{sp} \propto C^4 M^4 \text{ in } 0{\cdot}1\text{M Nacl}$$

where C is the HA concentration, M its molecular weight, and η_{sp} the intrinsic viscosity.

Conditions in our hylan–water systems are, therefore, at the most favourable for the formation of hydrogen-bonded chain–chain entanglement networks. The molecular weight is high ($> 4 \times 10^6$ Da), and the concentration also higher than it is possible to study rheologically ($> 10\%$). Structured into such networks, the water is bound and behaves quite different from free water. It must, therefore, be concluded that such a large capacity of HA entangled networks to build water into their structure is also responsible for their unusually high viscoelasticity after the onset of entanglement.

After the completion of our publication we observed a study on low molecular weight hyaluronic acid ($\sim 1{\cdot}50 \times 10^5$ Da) and certain of its esters (Joshi & Topp, 1992). In these samples, possibly due to the low molecular weight, they could not observe distinct phase transitions due to free water and freezing bound water. Neverthless, they were able to calculate the amount of non-freezing water ($13{\cdot}4 \pm 1{\cdot}7$), per disaccharide unit, which is in good agreement with our value of 13. This would be anticipated in view of the identical disaccharide building units in the two systems. These workers did not determine the amount of freezing-bound water associated with the non-esterified hyaluronic acid, and identify only total 'freezable water'.

ACKNOWLEDGEMENTS

The authors wish to thank Dr T. Hatakeyama and Dr H. Hatakeyama for their invaluable help and advice during the conduct of this work and in writing the paper, which was undertaken during the residence of one of us (GOP) in their laboratory. Dr Endre A. Balazs inspired this study and supplied the hylan used.

REFERENCES

Arnott, S., Mitra, A.K. & Raghunathan, S. (1983). *J. Mol. Biol.*, **169**, 861–72.

Balazs, E.A. (1968). *Univ. Mich. Med. Ctr. J.* (Suppl.), 255–9.

Balazs, E.A., Leshchiner A., Leshchiner, A. & Band, P. (1987). United States Patent No. 4, 713, 448.

Balazs, E.A., Leshchiner, A., Wedlock, D.J., Cowman, M., Band, P., Larsen, N., Leshchiner, A. & Hoefling, J. (1988). Biomatrix Report 101. Biomatrix Inc., Ridgefield, NJ, USA.

Balazs, E.A. & Denlinger, J.L. (1989). *CIBA Foundation Symposium 143; The Biology of Hyaluronan*, ed. D. Evered. Wiley & Sons, Chichester, 265–76.

Balazs, E.A. & Leshchiner, E.A. (1986). United States Patent No. 4, 582, 865.

Balazs, E.A. & Leshchiner, E.A. (1989). In *Cellulosics Utilisation*, eds H. Inagaki & G.O. Phillips. Elsevier Applied Science, London, pp. 233–41.

Bolliner, H. & Wik, O. (1987). *Acta Oto-Laryngol*, **442**, 25–30.

Davies, A., Gormaly, J., Wyn-Jones, E., Wedlock, D.J. & Phillips, G.O. (1982). *Intern. J. Biol. Macromol.*, **4**, 436–38.

Davies, A., Gormaly, J., Wyn-Jones, E., Wedlock, D.J. & Phillips, G.O. (1983). *Biochem. J.*, **213**, 363–9.

Fouissac, E. Milas, M., Rinaudo, M. & Borsali, R. (1992). *Macromolecules*, **25**, 5613.

Franks, F. (1972). *Water, A Comprehensive Treatise*, Vol. 1, ed. F. Franks. Plenum Press, New York, London, pp. 89–121.

Hatakeyama, T. & Nakamura, K. (1988). *Thermochimica Acta*, **123**, 153–61.

Hatakeyama, T., Nakamura, K., Yoshida, H. & Hatakeyama H. (1985*a*). *Thermochimica Acta*, **88**, 223–8.

Hatakeyama, H., Iwata, H. & Hatakeyama T. (1985*b*). In *Cellulose and Its Derivatives*, eds J.F. Kennedy, G.O. Phillips, D.J. Wedlock & P.A. Williams. Ellis Horwood, Chichester, p. 255.

Hatakeyama T., Nakamura, K., Yoshida, H. & Hatakeyama H. (1985*c*). *Thermochimica Acta*, **88**, 233.

Hatakeyama, T., Ikedo, Y. & Hatakeyama H. (1987*a*). In *Wood and Cellulosics*, eds J.F. Kennedy, G.O. Phillips & P.A. Williams. Ellis Horwood, Chichester, pp. 23–30.

Hatakeyama, T. Ikeda, Y. & Hatakeyama H. (1987*b*). *Makromol. Chem.*, **188**, 1875–84.

Hatakeyama, T., Yoshida, H. & Hatakeyama, H. (1987*c*). *Polymer*, **28**, 1232–6.

Hatakeyama, T., Yoshida, H. & Hatakeyama, H. (1987*d*). *Polymer*, **28**, 1282.

Hatakeyama, H., Iwata, H. & Hatakeyama T. (1987*e*). In *Wood and Cellulosics*, eds J.F. Kennedy, G.O. Phillips, & P.A. Williams. Ellis Horwood, Chichester, p. 23.

Joshi, H.N. & Topp, E.M. (1992). *Intern. J. Pharmaceutics*, **80**, 213–25.

Laurent, T.C. (1987). *Acta Oto-Laryngol*, **442**, 7–24.

Mauritz, K.A. & Fu, R.M. (1988). *Macromolecules*, **21**, 1324–33.

Morris, E.R., Rees, D.A. & Welsh, E.J. (1980). *J. Mol. Biol*, **138**, 383–400.

Nakamura, K., Hatakeyama, T. & Hatakeyama H. (1982). In *Wood and Cellulosics*, eds J.F. Kennedy, G.O. Phillips & P.A. Williams. Ellis Horwood, Chichester, pp. 97–104.

Nakamura, K., Hatakeyama, T. & Hatakeyama H. (1983). *Polymer*, **24**, 871.

Nakamura, K., Hatakeyama, T. & Hatakeyama, H. (1987). *Polymer*, **28**, 97.

Uedaira, H. (1975). *Hyomen*, **13**, 297–302.

Wise, W.B. & Pfeffer, P.E. (1987). *Macromolecules*, **20**, 1550–4.

Yanaki, T. & Yamaguchi, (1990). *Biopolymers*, **30** , 415.

Yoshida, H., Hatakeyama, T. & Hatakeyama H. (1989). In *Cellulose: Structural and Functional Aspects*, eds J.F. Kennedy, G.O. Phillips & P.A. Williams. Ellis Horwood, Chichester, pp. 305–16.

Yoshida, H., Hatakeyama, T. & Hatakeyama H. (1990). *Polymer*, **31**, 693–8.